NANOSYSTEMS:
PHYSICS, CHEMISTRY, MATHEMATICS

Filipov I., et al. *Nanosystems: Phys. Chem. Math.*, 2025, **16** (6), 778–784.
http://nanojournal.ifmo.ru
DOI 10.17586/2220-8054-2025-16-6-778-784

Original article

Heterodyne detection method of multimode states for subcarrier wave continuous variable quantum key distribution

Ilya Filipov[1,2,a], Roman Goncharov[1,b], Michael Dashkov[3,c], Ekaterina Bogdanova[3,d], Alexandr Zinovev[1,e], Vladimir Chistiakov[1,f], Fedor Kiselev[1,2,g]

[1]ITMO University, Saint Petersburg, Russia

[2]SMARTS-Quanttelecom LLC, Saint Petersburg, Russia

[3]Povolzhskiy State University of Telecommunications and Informatics (PSUTI), Samara, Russia

[a]imfilipov@itmo.ru, [b]rkgoncharov@itmo.ru, [c]m.dashkov@psuti.ru, [d]ei.bogdanova@psuti.ru, [e]avzinovev@itmo.ru, [f]v_chistyakov@itmo.ru, [g]fdkiselev@itmo.ru

Corresponding author: Ilya Filipov, imfilipov@itmo.ru

PACS 03.67.-a, 42.50.-p

ABSTRACT A novel coherent detection method for subcarrier wave (SCW) quantum states applied to continuous-variable quantum key distribution (CV-QKD) is presented. The proposed approach relies on repeated phase modulation at the receiver and spatial separation of the carrier and subcarrier frequency components. The resulting output is an intermediate frequency determined by the difference between the sender's and receiver's modulation frequencies. An analytical model of the detection output is developed through time-varying modulation using a classical method based on Bessel functions, and a comparative analysis with alternative heterodyne detection methods is provided. Experimental validation confirms the linear dependence of the output signal on the receiver's modulation frequency and the sender's modulation index in the small-modulation regime. Furthermore, the feasibility of the proposed method is demonstrated through the detection of discretely modulated signals using quadrature phase-shift keying (QPSK).

KEYWORDS coherent detection, subcarrier wave, continuous variable, quantum key distribution.

ACKNOWLEDGEMENTS The work was financially supported by the Russian Science Foundation (project No.24-11-00398)

FOR CITATION Filipov I., Goncharov R., Dashkov M., Bogdanova E., Zinovev A., Chistiakov V., Kiselev F. Heterodyne detection method of multimode states for subcarrier wave continuous variable quantum key distribution. *Nanosystems: Phys. Chem. Math.*, 2025, **16** (6), 778–784.

1. Introduction

Quantum key distribution (QKD) addresses the problem of securely distributing random number sequences between remote parties using quantum states. The two main approaches in QKD are discrete-variable and continuous-variable protocols [1]. Continuous-variable quantum key distribution (CV-QKD) utilizes coherent detection methods and does not require single-photon detectors, which are replaced by balanced detectors based on effective PIN photodiodes. CV-QKD offers several practical advantages: better scalability via integrated photonics [2–4], seamless integration into existing telecom infrastructure [5], and high secure key rates in metropolitan networks [6].

Coherent states in CV-QKD can be generated as single-mode [7] or multimode [8]. Among the latter, one can highlight that subcarrier wave (SCW) coherent quantum states demonstrate higher information capacity [9]. They could also be obtained through phase modulation with discrete [10] and Gaussian modulation [11] without altering the optical setup. The main challenge for SCW states in terms of CV-QKD is the detection method. Existing methods for SCW modulated states include conventional homodyne and heterodyne detection based on 3 dB optical couplers [9], as well as some unique methods based on repeated phase modulation or spectral separation of subcarriers with different phases [8]. The latter were approved through proof-of-concept experiments [10], and appear to enable the use of the carrier mode as a phase-stable local oscillator. These methods require either multiple active optical components or are difficult to implement because of the optical instability of the method.

In this work, we introduce a novel coherent heterodyne detection scheme that overcomes these limitations and paves the way toward a fully practical SCW CV-QKD. Our approach implements repeated phase modulation at the receiver and leverages a deliberate shift in the SCW modulation frequency to define the heterodyne intermediate frequency, thereby decoding both quadratures of the incoming quantum state. We validate this concept through numerical modeling and a proof-of-concept experiment using off-the-shelf fiber-optic components, demonstrating robust quadrature retrieval.

The remainder of this paper is organized as follows. Section 2 introduces the proposed detection method and compares it with previously developed methods. Section 3 presents a proof-of-concept experiment that demonstrates the feasibility of the approach. In Section 4, we discuss the results in the context of the underlying assumptions.

2. Detection principles

Coherent detection of SCW quantum states relies on mixing these states with a strong reference field, the local oscillator. The most common implementation implies the 3 dB coupler, which works for both single-mode and SCW coherent states [9].

Specific techniques have also been developed for SCW states [8, 10]. These exploit the strong carrier mode as a phase-stable local oscillator, made possible by Alice's low modulation index $m_A \ll 1$. One such approach applies repeated phase modulation on Bob's side, then separates carrier and subcarriers into different photodiodes of a balanced detector.

Fig. 1 shows a simplified scheme of this method, along with the optical power spectrum of the transmitted SCW signal. In the inset, we plot the balanced detector output voltage for various phase differences between modulators of Alice and Bob in a simplified form. Phase modulation distributes optical power between the carrier and subcarriers, with the relative phase setting the energy balance. A fiber Bragg grating filter and circulator isolate the carrier: the grating reflects a narrow spectral slice, which the circulator then directs to a second photodiode.

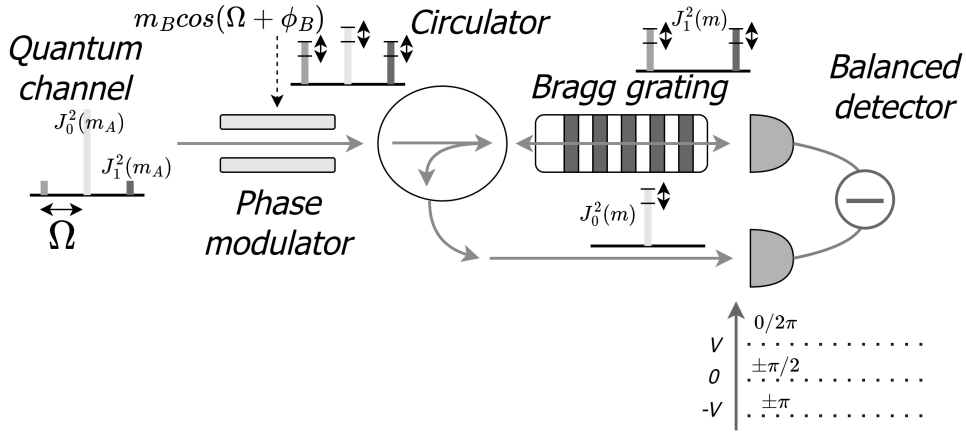

FIG. 1. SCW CV-QKD heterodyne detection based on repeated phase modulation. Top: optical power spectrum of SCW signal. Inset: balanced-detector voltage vs. phase difference

For identical modulation frequencies Ω and Alice's small index $m_A \ll 1$, the balanced detector output is

$$V = R(\lambda)GTE_0^2(1 - 2J_0^2(m)), \tag{1}$$

where $R(\lambda)$ is the photodiode responsivity at wavelength λ, G is the transimpedance gain, E_0 is the field amplitude before modulation, T is the combined channel and receiver transmittance, and J_0 is the zero-order Bessel function (from the Jacobi–Anger expansion), and m is the effective modulation index:

$$m = \sqrt{m_A^2 + m_B^2 + 2m_A m_B \cos\Delta\phi} \tag{2}$$

with m_A, m_B Alice's and Bob's indices and $\Delta\phi$ their phase difference. To balance the optical paths (and cancel the DC component), Bob's index m_B is set to approximately 1.13 [11]. This scheme supports both discrete [8] and Gaussian [11] modulation formats.

Unlike prior works where $\Delta\phi = \phi_A - \phi_B$ was static, we introduce a time dependence by letting $\phi_B(t) = \omega t + \phi_0$, so that

$$m(t) = \sqrt{m_A^2 + m_B^2 + 2m_A m_B \cos\left(\omega t - \phi_A(t) + \phi_0\right)}, \tag{3}$$

Shifting Bob's modulation frequency by ω (to $\Omega' = \Omega + \omega$) thus generates a heterodyne intermediate frequency encoding both quadratures.

Fig. 2 compares the analytical output of the balanced detector for three configurations: the proposed method, a coupler-based method utilizing an external reference field, and the configuration described in [10]. All three recover the intermediate frequency, though the proposed method shows a modest reduction in efficiency.

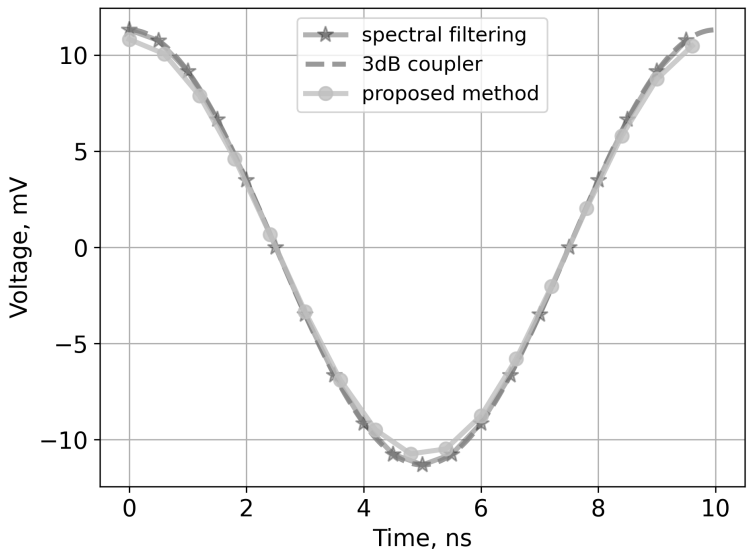

FIG. 2. Analytical comparison of balanced detector outputs for coupler-based heterodyne (dashed), spectral filtering [10] (solid), and the proposed method (dash-dotted)

3. Experimental setup

To validate the assumptions from Section 2, we assembled the experimental setup shown in Fig. 3. It comprises two modules: Alice and Bob. The Alice module includes a tunable Neophotonics laser source (linewidth < 100 kHz, central frequency 193.4 THz) as the optical carrier, a SMARTS - Quanttelecom lithium niobate phase modulator (10 GHz bandwidth) for SCW modulation, and a tunable optical attenuator to control the mean value of the output optical power. The Bob module consists of an identical phase modulator for receiver-side remodulation utilizing shifted modulation frequency and a Teraxion ClearSpectrum fiber Bragg grating filter (bandwidth < 7 GHz) aligned with the carrier frequency, coupled with an optical circulator to separate and route reflected carrier light to the second photodiode. Optical paths were matched by patch cord, and the balanced photodetector BPD-003 by General Photonics was utilized as a shot-noise limited detector with a 200 MHz bandwidth.

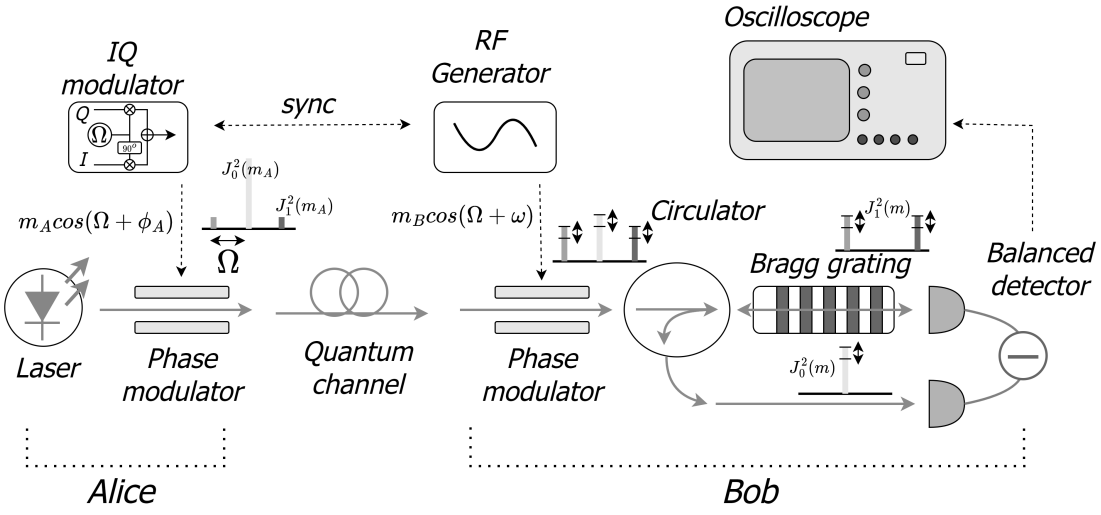

FIG. 3. Experimental setup for validating the SCW CV-QKD detection method

The electronics include a quadrature modulator to generate Alice's modulation signal and an RF generator to set a stable offset frequency on Bob's side. On Alice's side, the quadrature modulator was implemented using a combination of a RF source Rohde&Schwarz SGS100A and an I/Q modulation generator Rohde&Schwarz AFQ100B. The modulation frequency of the RF source was set at $\Omega = 4.8$ GHz. This frequency was selected based on the bandwidth of the fiber Bragg grating filter used on Bob's side. The SCW must fall within the stop band of the grating's reflection spectrum to allow effective spectral separation during detection. Therefore, for the filter used in the experiment, the doubled

modulation frequency 2Ω was required to be at least 9.5 GHz. On Bob's side, a modulation signal was generated using a programmable phase-locked loop (PLL) circuit, allowing for tunable modulation frequency. The synchronization of Alice's and Bob's modulation frequencies was achieved using a 100 MHz reference signal from the RF source to PLL through the wire. The reference clock distribution through the fiber channel, which is commonly employed in discrete-variable QKD systems based on subcarrier waves [12], was omitted in the experimental setup for the sake of simplicity.

The output of the balanced detector was recorded using a Rohde&Schwarz oscilloscope with 1 GHz bandwidth and 5 GSa/s sampling rate without analog filtering. The oscilloscope bandwidth exceeded the one of the balanced detector and the sampling rate provided sufficient oversampling relative to the detector bandwidth. All signal processing was performed offline using digital signal processing techniques.

First, we measured the intermediate frequency's dependence on Bob's remodulation frequency. The results of this measurement are presented in Fig.4. During the experiment, the output frequency of the PLL on the Bob's side was tuned from 4.810 GHz to 4.860 GHz, while all other parameters kept constant. Alice's modulation frequency was set to 4.800 GHz, and no digital I/Q modulation was applied. To analyze the relationship between the measured intermediate frequency and the Bob's modulation frequency, linear regression was employed. The coefficient of determination R^2 for the measured data was found to be approximately 0.999. The observed dependence appears to be linear and is consistent with the assumption presented in Section 2. Due to the frequency synchronization between Alice's and Bob's RF sources, the resulting intermediate frequency exhibited high stability.

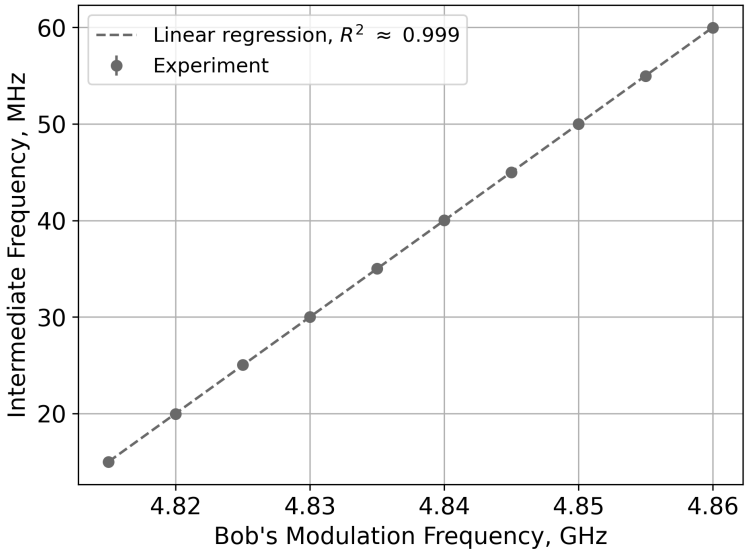

FIG. 4. Intermediate frequency vs. Bob's modulation frequency (Alice fixed at 4.8 GHz). Dots: experimental data; dashed line: linear fit

Second, we evaluated the amplitude linearity of the intermediate-frequency signal as a function of Alice's modulation index m_A in the small-index regime. Establishing linearity is crucial for the implementation of advanced modulation techniques such as Gaussian modulation, probability-shaped QAM, and APSK [13, 14]. The corresponding measurement results are presented in Fig. 5. During the experiment, Alice's modulation index was varied approximately from 0.11 to 0.25 by adjusting the amplitude of the RF source. As in the previous measurement, Alice's modulation frequency was fixed at 4.8 GHz, and digital I/Q modulation was not applied. In addition, Bob's modulation frequency was offset by 50 MHz relative to Alice's frequency to generate a detectable intermediate frequency. To analyze the relationship between Alice's modulation index and Bob's output amplitude, linear regression analysis was performed. The resulting coefficient of determination R^2 was approximately 0.994, indicating a strong linear relationship. This behavior is consistent with the assumptions outlined in Section 2 and further supports the feasibility of applying linear modulation schemes within the proposed detection method.

Finally, we implemented a QPSK modulation to demonstrate the feasibility of detecting discretely modulated SCW signals using the proposed detection method. The modulation sequence was set using the Rohde&Schwarz AFQ 100B signal generator. The symbol rate was set to 1 MHz, and Alice's modulation index m_A was configured to 2.2×10^{-3}. The modulation frequencies of Alice and Bob were fixed at 4.800 GHz and 4.825 GHz, respectively. Fig. 6 shows the result of signal demodulation at the output of the balanced detector. The demodulation process was performed in the digital domain using a digital down-conversion (DDC) scheme. The intermediate frequency signal was subjected to band-pass filtering to isolate the relevant spectral component. This was followed by frequency down-conversion using a digital local oscillator and low-pass filtering to extract the baseband signal. Then, the sampling rate was reduced to match the symbol

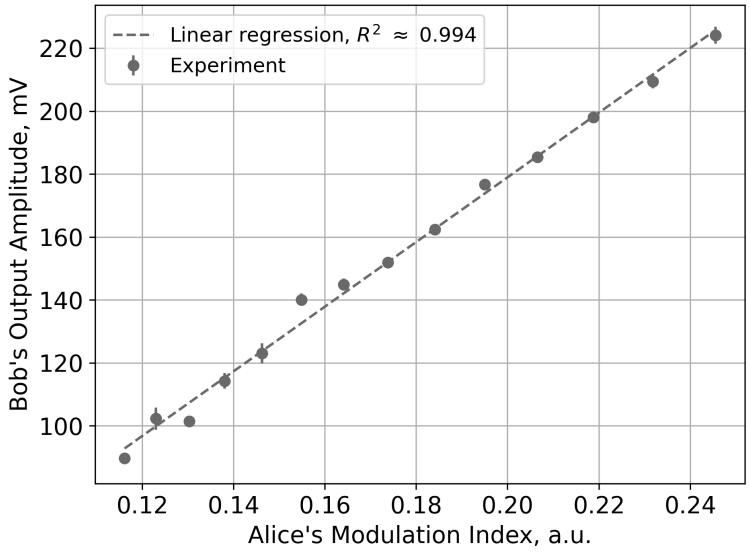

FIG. 5. Intermediate-frequency amplitude vs. Alice's modulation index. Dots: experimental data; dashed line: linear fit

rate. The mapping between the received signal phases and symbol states was performed based on prior knowledge of the transmitted QPSK constellation.

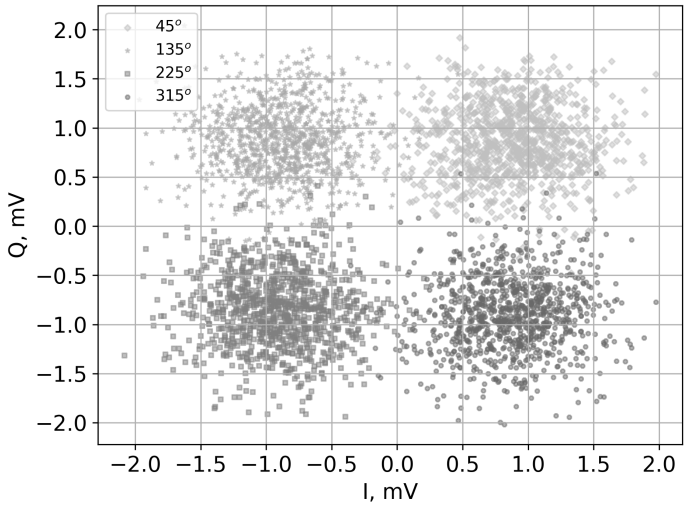

FIG. 6. Constellation diagram of SCW-modulated QPSK at the balanced detector output after digital down-conversion

4. Discussion and conclusion

We have presented a novel detection method for SCW-modulated states through time-varying modulation using a classical method based on Bessel functions. The proposed method produces an output functionally equivalent to established heterodyne techniques while employing a phase-stable approach based on repeated phase modulation. We experimentally demonstrated the reconfigurability of the intermediate frequency and a linear dependence of the output amplitude on Alice's modulation index. As a proof-of-concept, we transmitted and detected a QPSK-modulated signal using this method.

The proposed detection technique addresses several limitations associated with previously reported heterodyne and dual-homodyne detection schemes [10, 11]. Dual-homodyne detection requires a larger number of components compared to standard homodyne detection, including a balanced detector, a phase modulator, and a narrowband fiber Bragg grating filter. This not only increases the cost and complexity of implementation but also introduces additional technical challenges, such as the need for multiple control signals and precise spectral alignment of the fiber Bragg grating filters. In

contrast, the proposed detection scheme neither increases the number of optical components relative to a homodyne setup nor requires fiber Bragg grating filter alignment in Bob's module.

The heterodyne detection method described in [10] relies on matching the filter transmission spectrum with the laser carrier frequency along the slope of the transmission curve. Under this condition, the carrier power is split approximately equally between the reflected and transmitted ports of the fiber Bragg filter. In SCW CV-QKD detection architectures, both the carrier frequency and the filter transmission spectrum are generally sensitive to operational variations in systems employing narrowband filters. Furthermore, the rate of change of the transmission for the central carrier frequency is higher when it lies on the slope of the transmission spectrum than at its peak. This can lead to additional power fluctuations and, in cases of strong variations, to the saturation of one arm of the balanced detector. Positioning the carrier frequency at the transmission peak in the proposed scheme effectively mitigates this source of instability.

Nevertheless, several technical challenges remain before realizing a fully functional SCW CV-QKD system. These challenges span both digital signal processing (DSP) and physical-layer implementation.

First, existing DSP techniques used in single-mode CV-QKD systems [15] must be adapted for the Alice and Bob modules. For example, our experiment omitted pulse shaping on Alice's side to simplify modulation. However, incorporating pulse shaping could confine the modulation spectrum and enable matched filtering via a root-raised-cosine filter.

Second, physical-layer constraints must be addressed. CV-QKD schemes with a transmitted local oscillator require high LO power for shot-noise-limited detection, which can introduce excess noise [16]. The SCW approach offers strong spectral separation between the quantum signal and LO, potentially improving isolation. Conversely, achieving high carrier power relative to subcarriers necessitates a lower Alice modulation index, which may demand specialized hardware solutions.

Finally, the security of the physical implementation must also be carefully considered. Numerous side-channel attacks have been reported for systems based on single-mode states [17], and the relevance of such vulnerabilities to SCW CV-QKD architectures must be systematically evaluated.

References

[1] Pirandola S., Andersen U. L., Banchi L., Berta M., Bunandar D., Colbeck R., Englund D., Gehring T., Lupo C., Ottaviani C., Pereira J.L., Razavi M., Shamsul Shaari J., Tomamichel M., Usenko V.C., Vallone G., Villoresi P., and Wallden P. Advances in quantum cryptography. *Advances in optics and photonics*, 2020, **12**(4), P. 1012–1236.

[2] Zhang G., Haw J.Y., Cai H., Xu F., Assad S., Fitzsimons J.F., Zhou X., Zhang Y., Yu S., Wu J., Ser W. An integrated silicon photonic chip platform for continuous-variable quantum key distribution. *Nature Photonics*, 2019, **13**(12), P. 839–842.

[3] Hajomer A.A. , Bruynsteen C., Derkach I., Jain N., Bomhals A., Bastiaens S., Andersen U.L., Yin X., and Gehring T. Continuous-variable quantum key distribution at 10 gbaud using an integrated photonic-electronic receiver. *Optica*, 2024, **11**(9), P. 1197–1204.

[4] Piétri Y.,Trigo Vidarte L., Schiavon M., Vivien L., Grangier P., Rhouni A., and Diamanti E. Experimental demonstration of continuous-variable quantum key distribution with a silicon photonics integrated receiver. *Optica Quantum*, 2024, **2**(6), P. 428–437.

[5] Hajomer A.A., Derkach I., Usenko V.C., Andersen U.L., and Gehring T. Coexistence of continuous-variable quantum key distribution and classical data over 120-km fiber. *arXiv preprint arXiv:2502.17388*, 2025.

[6] Milovančev D., Vokić N., Laudenbach F., Pacher C., Hübel H., and Schrenk B. High rate cv-qkd secured mobile wdm fronthaul for dense 5 g radio networks. *Journal of Lightwave Technology*, 2021, **39**(11), P. 3445–3457.

[7] Zhang Y., Bian Y., Li Z., Yu S., and Guo H. Continuous-variable quantum key distribution system: Past, present, and future. *Applied Physics Reviews*, 2024, **11**(1).

[8] Samsonov E., Goncharov R., Gaidash A., Kozubov A., Egorov V., and Gleim A. Subcarrier wave continuous variable quantum key distribution with discrete modulation: mathematical model and finite-key analysis. *Scientific Reports*, 2020, **10**(1), P. 10034.

[9] Su Z., Wang J., Cai D., Guo X., Wang D., and Li Z. Experimental demonstration of phase sensitive multimode continuous variable quantum key distribution with improved secure key rate. *Photonics Research*, 2023, **11**(11).

[10] Samsonov E., Goncharov R., Fadeev M., Zinoviev A., Kirichenko D., Nasedkin B., Kiselev A., and Egorov V. Coherent detection schemes for subcarrier wave continuous variable quantum key distribution. *Journal of the Optical Society of America B: Optical Physics*, 2021, **38**(7), P. 2215–2222.

[11] Goncharov R., Kiselev A., Samsonov E., and Egorov V. Subcarrier wave continuous-variable quantum key distribution with gaussian modulation: composable security analysis. *Computer Optics*, 2023, **47**(3), P. 374–380.

[12] Gleim A.V., Egorov V.I., Nazarov Y.V., Smirnov S.V., Chistyakov V.V., Bannik O.I., Anisimov A.A., Kynev S.M., Ivanova A.E., Collins R.J., Kozlov S.A., and Buller G.S. Secure polarization-independent subcarrier quantum key distribution in optical fiber channel using bb84 protocol with a strong reference. *Optics Express*, 2016, **24**(3), P. 2619–2633.

[13] Pereira D., Almeida M., Facao M., Pinto A.N., and Silva N.A. Probabilistic shaped 128-apsk cv-qkd transmission system over optical fibres. *Optics Letters*, 2022, **47**(15), P. 3948–3951.

[14] Roumestan F., Ghazisaeidi A., Renaudier J., Vidarte L. T., Leverrier A., Diamanti E., and Grangier P. Shaped constellation continuous variable quantum key distribution: Concepts, methods and experimental validation. *Journal of Lightwave Technology*, 2024, **42**(15), P. 5182–5189.

[15] da Silva V.L., Dias M.A., Neto N.A.F., and Tacla A.B. From coherent communications to quantum security: Modern techniques in cv-qkd. Proceedings of the Conference "2024 SBFoton International Optics and Photonics Conference (SBFoton IOPC)", Salvador, Brazil, 2024, P. 1–5.

[16] Qi B., Huang L.-L., Qian L., and Lo H.-K. Experimental study on the gaussian-modulated coherent-state quantum key distribution over standard telecommunication fibers. *Physical Review A–Atomic, Molecular, and Optical Physics*, 2007, **76**(5), P. 052323.

[17] Nasedkin B., Goncharov R., Morozova P., Filipov I., Chistiakov V., Samsonov E., and Egorov V. Quantum hacking on the technical implementation of continuous-variable quantum key distribution systems. *Radiophysics and Quantum Electronics*, 2025, **67**(1), P. 23–37.

Submitted 02 October 2025; revised 01 November 2025, 12 November 2025; accepted 13 November 2025

Information about the authors:

Ilya Filipov – ITMO University, 199034, Saint Petersburg, Kadetskaya Line 3k2, Russia; SMARTS-Quanttelecom LLC, 199178, Saint Petersburg, Vasilievsky island 6 Line 59, Russia; ORCID 0000-0003-4564-8284; imfilipov@itmo.ru

Roman Goncharov – ITMO University, 199034, Saint Petersburg, Kadetskaya Line 3k2, Russia; ORCID 0000-0002-9081-8900; rkgoncharov@itmo.ru

Michael Dashkov – Povolzhskiy State University of Telecommunications and Informatics (PSUTI), 443010, Samara, Moskovskoe Shosse St., 77, Russia; ORCID 0000-0002-3919-4151; m.dashkov@psuti.ru

Ekaterina Bogdanova – Povolzhskiy State University of Telecommunications and Informatics (PSUTI), 443010, Samara, Moskovskoe Shosse St., 77, Russia; ei.bogdanova@psuti.ru

Alexandr Zinovev – ITMO University, 199034, Saint Petersburg, Kadetskaya Line 3k2, Russia; ORCID 0000-0003-0789-998X; avzinovev@itmo.ru

Vladimir Chistiakov – ITMO University, 199034, Saint Petersburg, Kadetskaya Line 3k2, Russia; ORCID 0000-0002-2414-3490; v_chistyakov@itmo.ru

Fedor Kiselev – ITMO University, 199034, Saint Petersburg, Kadetskaya Line 3k2, Russia; SMARTS-Quanttelecom LLC, 199178, Saint Petersburg, Vasilievsky island 6 Line 59, Russia; ORCID 0000-0002-3894-511X; fdkiselev@itmo.ru

Conflict of interest: the authors declare no conflict of interests.